Robust Identification of Non-linear Greenhouse Model using Evolutionary Algorithms

J.M. Herrero, X. Blasco, M. Martínez, C. Ramos, J. Sanchis

Department of Systems Engineering and Control, Polytechnic University of Valencia, Camino de Vera s/n, 46022 Valencia, Spain;

Tel.: +34-96-3879571, Fax: +34-96-3879579

e-mail of corresponding author: juaherdu@isa.upv.es

Abstract

This paper presents the non-linear modelling, based on first principle equations, for a climatic model of a greenhouse and the estimation of the feasible parameter set (FPS) when the identification error is bounded simultaneously by several norms. The robust identification problem is transformed into a multimodal optimization problem with an infinite number of global minima that constitute the FPS. For the optimization task, a special evolutionary algorithm ($\epsilon-$GA) is presented, which characterizes the FPS by means of a discrete set of models that are well distributed along the FPS. A procedure for determining the norm bounds, such that $FPS \neq \emptyset$, is presented.

Key words: Robust Identification, Multimodal Optimization, Multiobjective Optimization, Evolutionary Algorithms, Greenhouse Modelling.

1 Introduction

Climate control is increasingly necessary for precision agriculture that produces more and better crops. In recent years, it has become possible to begin developing and applying systems with more sophisticated control strategies - thanks to the application of modelling and identification techniques (Rodríguez, Yebra, Berenguel and Dormido, 2002; Boaventura, 2003).

The problems involved in controlling greenhouses are strongly dependent on the geographical area. Solutions that are valid in some regions must be adapted or changed to fit others. More particularly, in Mediterranean countries the high levels of radiation, temperature, and humidity during summer are factors that differentiate this region from other European regions. Under these conditions, conventional temperature control is insufficient and must be complemented with humidity control. For instance, a sudden fall in humidity would produce a high crop transpiration, followed by water stress that would damage crop production and quality (Baille, Baille and Delmon, 1994).

Therefore, to keep both temperature and humidity inside a desired range, a window opening and fog system must be correctly controlled and this creates the need for multivariable controllers (Blasco, Martínez. Herrero, Ramos and Sanchis, 2007). The required multivariable process is non-linear and influenced by biological processes. Developing a suitable mathematical model, as well as an adequate adjustment of the model parameters, is a complex task.

Because the process behaviour is incompletely known and that available data is insufficient or unreliable, the identified parameters will contain uncertainties. This factor must be considered when the model is used for prediction,

controller design, and so on. The task of identifying the nominal model, and its uncertainty, is called robust identification (RI).

Two different approaches are possible in RI: stochastic or deterministic. In the first, the identification error (IE), meaning the difference between the process output measurements and the model simulated outputs, is assumed to be modelled as a random variable with several statistical properties. Under this approach, it is possible to use classical identification techniques (Walter and Pronzalo, 1997; Ljung, 1999) to obtain the nominal model and its uncertainty - which is related to the covariance matrix of the estimated parameters. When these assumptions do not work, the deterministic approach may be more appropriate (Walter and Piet-Lahanier, 1990; Milanese, Norton, Piet Lahanier and Walter, 1996; Reinelt, Garulli and Ljung, 2002), where the identification error, although unknown, is assumed to be bounded.

The objective of the deterministic approach is to obtain the nominal model and its uncertainty - or directly the feasible parameter set (FPS); i.e. the parameter set that keeps the IE bounded for certain IE functions or norms and their bounds.

When the model has linear parameters, the FPS is, if it exists, a convex polytope. This polytope may be complex because the number of vertices can grow exponentially as the number of observations increases, and so the complexity involved in obtaining the polytope can be considerable. The polytope is often approximated using orthotopes (Belforte, Bona and Cerone, 1990), ellipsoids (Fogel and Huang, 1982), or parallelotopics (Chisci, Garulli, Vicino and Zappa, 1998); and these generally result in a more conservative characterization of the FPS.

When the model is non-linear, the FPS may be a non-convex, and even disjoint, polytope - and this makes it more difficult to find a tight characterization of the FPS. Some techniques: such as interval computation (Walter and Kieffer, 2003); support vector machine (Keesman and Stappers, 2004); signomial programming (Milanese and Vicino, 1991); and others (see an overview in Keesman (2003)) can be used. However, these techniques suffer limitations (the type of function for bounding the IE, the inability to characterize a non-convex or disjoint FPS), or their use is complicated when the model is complex (non-differentiable with respect to its parameters, discontinuities in parameters and/or signals, etc.).

To overcome these handicaps, a more flexible and general methodology for characterizing FPS is presented. It can identify many processes and characterize convex, non-convex, and even disjoint FPS. In addition, several norms can be taken into account at the same time. This enables, for instance, bounding the IE for each experimental sample and its integral simultaneously; as well as the consideration of independent norms for each output. The practical sense of simultaneous norms is justified: for example, it would be useful if the model predictions attempt to satisfy a limited maximal error, (∞-norm) and - at the same time - find a good average fitting between model and experiment (absolute norm).

The proposed methodology is based on the optimization of a function that is built from selected IE norms and bounds. This function may have the result that in the global minima search space there are points belonging to the FPS contour which could be used to characterize the FPS. This would be a multimodal function, which could be non-convex and/or present local minima, and so classical optimizers (for example, SQP) are inappropriate.

The FPS depends on the norms used to bound the IE; and especially, their corresponding bounds. To select the bounds, a priori process knowledge and noise characteristics must be used. However, this can be a difficult task, because the bound is often selected by taking into account the desired performance for the model prediction. Low values for the bounds could result in an empty FPS; whereas high values could provide a more conservative FPS; and so IE bound selection is a critical decision.

A procedure which uses Pareto front information will be proposed to select bounds and avoid an $FPS = \emptyset$. This front is obtained by the simultaneous minimization of the IE norms, using a multiobjective optimization (MO).

This article will present the capabilities of the proposed methodology using the RI of a non-linear greenhouse climate model with real data from a summer in the Mediterranean area. The main capabilites shown are: flexibility; demonstrated by the fact that four norms are applied simultaneously on indoor temperature and humidity; and power; demonstrated by the fact that the model contains hard non-linearities.

The work is organized as follows. In section 2, the fundamentals of the ϵ-GA multimodal optimization algorithm and the algorithm itself are presented. The proposed RI methodology is shown in section 3. Sections 4 shows an example of modelling and section 5 shows RI in a greenhouse climate model. The main conclusions are presented in section 6.

2 ϵ-GA evolutionary algorithm

ϵ-GA (Herrero, 2006) is an evolutionary strategy (ES) (Bäck and Schwefel, 1995), inspired by multiobjective EAs (MOEA) (Coello, Veldhuizen and Lamont, 2002), and designed to optimize those multimodal mono-objective functions which have an infinite number of global optima. ϵ-GA uses both an archive $A(t)$ to store a set of minimal solutions that take active part in the algorithm evolution; and a "restart and phased" procedure (Ursem, 2002) to avoid premature convergence. This final characteristic distinguishes it from classical ES.

2.1 Related concepts of the ϵ-GA

The optimization problem consists of:

Definition 1 *(Global minimum set). Given a finite L-dimensional domain $D \subseteq \mathcal{R}^L$, $D \neq \emptyset$ and a function to optimize $J : D \rightarrow \mathcal{R}$, the set Θ^* will be the global minimum set of J if, and only if, Θ^* contains all the global optima of J.*

$$\Theta^* := \{\theta \in D : J(\theta) = J^*\},$$

being J^* a global minimum of J for the search space D.

From this definition, Θ^* is assumed to be a unique set which can contain infinite global optima and therefore, the best course of action is to obtain a finite set Θ^*_ϵ, in the solution space D, as a discretized approximation to Θ^*. To achieve this, the solution space is divided into a grid with ϵ_i width for each

dimension $i \in [1 \dots L]$ and the algorithm is forced to produce just one solution for each box. So, thanks to the grid, the solutions in Θ^*_ϵ are forced to be well distributed and to characterize Θ^* (see figure 1).

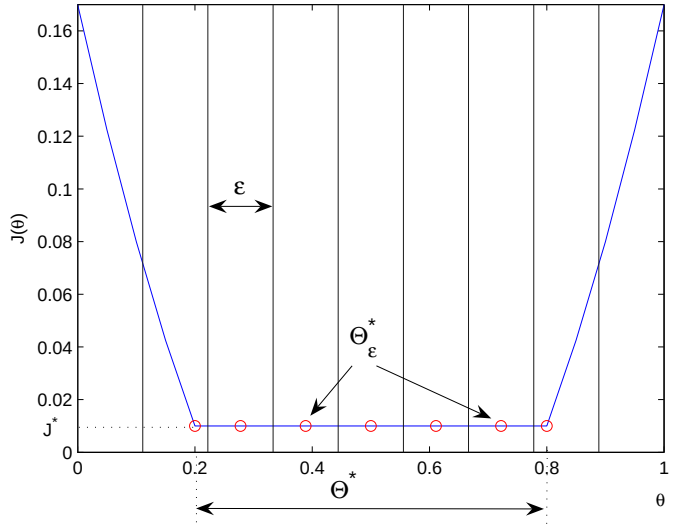

Figure 1. Multimodal optimization example. $L = 1$, $D \in [0 \dots 1]$, $n\_box = 9$ is the number of boxes in which search space is divided and so the box width is $\epsilon = 1/9$, $J^* = 0.01$ and $\Theta^* := \{\theta \in [0.2 \dots 0.8]\}$. A possible Θ^*_ϵ is represented by means of $\circ$. Note that inside the box, the solution nearest to its centre is preferred - so improving the characterization.

Concepts such as approximation and discretization must be specified to obtain Θ^*_ϵ, and so definitions of quasi-global minimum and box representation are shown next.

Definition 2 (Quasi-global minimum) Given a finite domain $D \neq \emptyset$ and a function to optimize $J : D \rightarrow \mathcal{R}$, the solution θ is considered as a quasi-global minimum of J, if and only if,

$$J(\theta) \leq J^* + \delta,$$

being $\delta > 0$ and J^* the global minimum value of J.

So, a global minimum solution is also a quasi-global minimum solution.

Definition 3 (Quasi-global minimum set). Given a finite domain $D \neq \emptyset$ and a function to optimize $J : D \to \mathcal{R}$, the set Θ^{**} will be the quasi-global minimum set of J if Θ^{**} contains all the quasi-global minimum solutions of J.

$$\Theta^{**} := \{\theta \in D : J(\theta) \leq J^* + \delta\},$$

being J^* a global minimum of J for the search space D and $\delta > 0$.

Definition 4 (Box). Given a vector $\theta = [\theta_1 \dots \theta_i \dots \theta_L] \in D \subseteq \mathcal{R}^L$ and the width box $\epsilon = [\epsilon_1 \dots \epsilon_i \dots \epsilon_L]$, its box is defined as the vector $\mathbf{box}(\theta) = [box_1(\theta) \dots box_i(\theta) \dots box_L(\theta)]$ where:

$$box_i(\theta) = \left\lfloor \frac{\theta_i - \theta_i^{min}}{\epsilon_i} \right\rfloor, \quad \epsilon_i > 0 \quad \forall i \in [1 \dots L].$$

So $box_i(\theta) \in [0 \dots (n\_box_i - 1)]$, being n_box_i the number of divisions of the grid in the dimension i

$$n\_box_i = \left\lceil \frac{\theta_i^{max} - \theta_i^{min}}{\epsilon_i} \right\rceil, \quad (\theta_i^{max} - \theta_i^{min}) \geq \epsilon_i$$

where θ_i^{max} and θ_i^{min} determine the limits of the solution space D.

Definition 5 (Box-representation). Given two vectors θ^1, $\theta^2 \in D$, whose images in the space of the function J are $J(\theta^1)$ and $J(\theta^2)$ respectively, it can be said that θ^1 *box*-represents θ^2 (denoted by $\theta^1 \preceq \theta^2$) for a certain $\epsilon_i > 0$ if

$$\mathbf{box}(\theta^1) = \mathbf{box}(\theta^2) \wedge J(\theta^1) \leq J(\theta^2).$$

Therefore, Θ^*_ϵ can be defined as:

Definition 6 (ϵ-global minimum set). Given a solution set Θ in the solution

space, the set $\Theta_\epsilon^* \subseteq \Theta$ will be an ϵ global minimum set of Θ, if and only if,

(1) It only contains quasi-global minimum solutions of Θ

$$\Theta_\epsilon^* \subseteq (\Theta \cap \Theta^{**}).$$

(2) Any vector in $\Theta \cap \Theta^{**}$ has a *box*-representation in Θ_ϵ^*, that is:

$$\forall \theta \in \Theta \cap \Theta^{**}, \;\; \exists \theta^* \in \Theta_\epsilon^* : \theta^* \preceq \theta.$$

Therefore, given a set Θ, Θ_ϵ^* must not be a unique set, because global minimum solutions of Θ which share the same box can *box* represent each other.

Definition 7 ($\Phi_\epsilon(\Theta)$ set). The set of all the ϵ global minimum sets of Θ will be called as $\Phi_\epsilon(\Theta)$.

With these definitions, it is possible to establish the procedure to manage the contents of the archive $A(t)$ (where Θ_ϵ^* is stored). So, it is necessary to know the global minimum J^*, although this is not always possible. The best approximation to J^* that the algorithm can provide is $J_\Theta^{min} = \min_{\theta \in \Theta} J(\theta)$.

Definition 8 (Inclusion of θ in $A(t)$) Given a vector θ in the solution space, δ (the parameter related to the quasi-global minimum solution, see definition 2) and the archive $A(t)$, θ will be included in the archive if, and only if,

$$J(\theta) \leq J_{A(t)}^{min} + \delta \tag{1}$$

$$\wedge$$

$$\neg \exists \theta^* \in A(t) : \theta^* \preceq \theta. \tag{2}$$

Being $J_{A(t)}^{min}$ the best solution included in $A(t)$. At the same time, the inclusion of θ in the archive could modify $J_{A(t)}^{min}$, and so all the solutions $\theta^* \in A(t)$ satisfying the following condition will be removed from $A(t)$.

$$J(\theta^*) > J^{min}_{A(t)} + \delta \tag{3}$$

$$\vee$$

$$\theta \preceq \theta^*. \tag{4}$$

Due to the inclusion procedure of the definition 8 the contents of $A(t)$ converge towards an ϵ-global minimum set (see demonstrations in Herrero (2006)).

Finally, the effect of parameters ϵ_i and δ is described. Coefficients ϵ_i show the desired discretization degree to apply to Θ^*_ϵ and it is directly related to the parameter physical meaning which defines the search space dimensions. The lower ϵ_i is, the higher n_box_i, and the solution numbers $|\Theta^*_\epsilon|$ are.

$$|\Theta^*_\epsilon| \leq \prod_{i=1}^{L} n\_box_i. \tag{5}$$

The parameter δ plays two roles related to convergence and diversity:

- A value $\delta \simeq 0$ improves the convergence and $\Theta^*_\epsilon \Rightarrow \Theta^*$, but worsens the approximation of Θ^* and so its characterization.
- On the contrary, a too high value of δ could cause the quasi-global minimum solutions of Θ^*_ϵ to be distorted Θ^* instead of characterizing it.

So, a good procedure to choose δ consists of starting from a value $\delta = \delta_{ini}$ and modifying it (for instance, by using a decreasing exponential function) towards a value $\delta = \delta_{fin}$ that is low enough to make the quasi-global minimum solutions be close to the global minimum solutions. Since δ will be decreasing, the properties of the inclusion procedure (definition 8) will remain unaltered and $A(t) \in \Phi(\Theta)$.

2.2 ϵ-GA description

The objective of the ϵ-GA algorithm is to provide an ϵ-global minimum set, Θ_ϵ^*. ϵ-GA uses the populations $P(t)$, $A(t)$ y $G(t)$.

(1) $P(t)$ is the main population and it explores the search space D. The population size is $Nind_P$.

(2) $A(t)$ is the archive where Θ_ϵ^* is stored. Its size $Nind_A$ is variable but bounded (equation (5)).

(3) $G(t)$ is an auxiliary population used to store the new individuals generated at each iteration by the algorithm. The population size is $Nind_G$.

The pseudocode of the ϵ-GA algorithm is given by:

```
1. t:=0
2. A(t):=∅
3. P(t):=ini_random(D)
4. eval(P(t))
5. A(t):=store(P(t),A(t))
6. mode:=exploration
7. while t<t_max do
8.      G(t):=create(P(t),A(t))
9.      eval(G(t))
10.     A(t+1):=store(G(t),A(t))
11.     P(t+1):=update(G(t),P(t))
12.     mode:=determinemode(P(t))
13.     t:=t+1
14. end while
```

The main steps of the above algorithm are detailed below:

Step 3. Population $P(0)$ is initialized with $Nind_P$ individuals, randomly created inside the search space D.

Steps 4 and 9. Function *eval* calculates the value of the fitness function $J(\theta)$ for each individual θ from $P(t)$ (step 4) or $G(t)$ (step 9).

Step 12. The function *determine mode* selects the algorithm operation mode between the exploration and exploitation modes. These modes affect how new individuals are created (function create). When the population $P(t)$ has converged, the exploitation mode must be selected, by using the difference between the best value $J^{min}_{P(t)} = \min_{\theta \in P(t)} J(\theta)$ and the worst value $J^{max}_{P(t)} = \max_{\theta \in P(t)} J(\theta)$ at iteration t. If $J^{max}_{P(t)} - J^{min}_{P(t)} < \delta$ the *exploitation* mode [1] will be selected, on the contrary, the *exploration* will be selected.

Step 5 and 10. Function *store* analyzes whether each individual of $P(t)$ (step 5) or $G(t)$ (step 10) must be included in archive $A(t)$. The individual will have to satisfy the inclusion condition (definition 8), and according to this definition other individuals will be removed. When including a new individual θ^1 in the archive, if its box ($\mathbf{box}(\theta^1)$) is occupied by another individual θ^2 from the archive, that is $\mathbf{box}(\theta^1) = \mathbf{box}(\theta^2)$, and $J(\theta^1) = J(\theta^2)$, the individual nearest to the centre of the box will be included [2] .In this way, a better distribution of the solutions inside the archive is achieved.

Step 8. Function *create* creates new individuals and stores them in population $G(t)$ using the following procedure until $G(t)$ is full:

[1] If $J^{min}_{P(t)} = J^*$ all the individuals in $P(t)$ will be quasi-global minimum solutions.
[2] Strictly according to definition 8, the individual θ^2 will not be included.

(1) Two individuals are randomly selected, θ^{p1} from $P(t)$, and θ^{p2} from $A(t)$.

(2) If the algorithm operates in *exploration* mode θ^{p2} is not altered, whereas in *exploitation*, it is mutated according to $\theta_i^{p2} = \theta_i^{p2} + N(0, \beta_{ini})$.

(3) A random number $u \in [0 \dots 1]$ is selected. If $u > P_{c/m}$ (crossover-mutation probability) step 4 is taken, otherwise, step 5.

(4) θ^{p1} and θ^{p2} are crossed over by the extended linear recombination technique and two new individuals θ^{h1} and θ^{h2} are created [3]:

$$\theta_i^{h1} = \alpha_i(t) \cdot \theta_i^{p1} + (1 - \alpha_i(t)) \cdot \theta_i^{p2}, \;\; \theta_i^{h2} = (1 - \alpha_i(t)) \cdot \theta_i^{p1} + \alpha_i(t) \cdot \theta_i^{p2}.$$

(5) θ^{p1} and θ^{p2} are mutated by random mutation with gaussian distribution [4].

$$\theta_i^{h1} = \theta_i^{p1} + N(0, \beta 1_i(t)), \;\; \theta_i^{h2} = \theta_i^{p2} + N(0, \beta 2_i(t)).$$

Step 11. Function *update* updates $P(t)$ with individuals from $G(t)$. One individual θ^G from $G(t)$ will be inserted in $P(t)$ replacing θ^p, if $J(\theta^G) < J(\theta^p)$ being $\theta^p = \arg\max_{\theta \in P(t)} J(\theta)$ so, the contents of $P(t)$ are converging.

Finally, when $t = t_{max}$, the individuals included in the archive $A(t)$ will be the solution Θ_ϵ^* to the multimodal optimization problem, being Θ the set of individuals generated by steps 3 and 8, that is,

$$\Theta = P(0) \bigcup \left(\bigcup_{0 \le \tau < t_{max}-1} G(t) \right), \quad \Theta \cap \Theta^* \neq \emptyset.$$

[3] $\alpha_i(t)$ is a random value with uniform distribution $\in [-d(t), 1 + d(t)]$ and $d(t)$ is a parameter tuned by a decreasing exponential function. $d(t) = \frac{d_{ini}}{\sqrt{1+\left((d_{ini}/d_{fin})^2-1\right)(t/(t_{max}-1))}}$.

[4] Variances $\beta 1_i(t)$ and $\beta 2_i(t)$ are expressed in percentage of $(\theta_{i\,max} - \theta_{i\,min})$ and are tuned by a function similar to the function used for tuning $d(t)$.

3 RI problem statement

The technique is based on the acceptance of an initial model structure, for instance, a series of first-order differential equations which can be obtained from physical principles.

$$\dot{\mathbf{x}}(t) = f(\mathbf{x}(t), \mathbf{u}(t), \theta) \tag{6}$$

$$\hat{\mathbf{y}}(t, \theta) = g(\mathbf{x}(t), \mathbf{u}(t), \theta) \tag{7}$$

where: $f(.), g(.)$ are the non-linear functions of the model; $\theta \in D \subset R^L$ is the vector [5] of unknown model parameters and $\mathbf{x}(t) \in R^n$, $\mathbf{u}(t) \in R^m$ and $\hat{\mathbf{y}}(t, \theta) \in R^l$ are the vector of model states, inputs, and outputs respectively.

Normally, the objective is to look for the best parameters, such as the model outputs (obtained by simulation using these parameters), which are as similar as possible to the real process parameters (obtained by experiments). This objective is achieved by a minimization of a function which penalizes the IE.

Definition 9 (Identification Error) The identification error $\mathbf{e}_j(\theta)$ for the output $j \in [1 \dots l]$ is stated:

$$\mathbf{e}_j(\theta) = \mathbf{y}_j - \hat{\mathbf{y}}_j(\theta),$$

where: $\mathbf{y}_j = [y_j(t_1), y_j(t_2) \dots y_j(t_N)]$ are the process output j measurements [6] when the inputs $\mathbf{U} = [\mathbf{u}(t_1), \mathbf{u}(t_2) \dots \mathbf{u}(t_N)]$ are applied to the model and $\hat{\mathbf{y}}_j(\theta) = [\hat{y}_j(t_1, \theta), \hat{y}_j(t_2, \theta) \dots \hat{y}_j(t_N, \theta)]$ are the simulated model output j when

[5] θ, $\mathbf{x}(t)$, $\mathbf{u}(t)$ e $\hat{\mathbf{y}}(t, \theta)$ are all column vectors

[6] $\mathbf{y}(t) \in \mathcal{R}^l$ is the column vector of process outputs.

the same inputs $\mathbf{U}$ are applied to the model [7].

It is assumed that the IE can be bounded by several norms [8] simultaneously.

Definition 10 (IE norm) Let N_i denote the p norm of the identification error vector for the output j as:

$$N_i(\theta) = \|\mathbf{e}_j(\theta)\|_p, \quad i \in A := [1, 2, \ldots, s],$$

where s is the number of norms [9].

Therefore, there exists an FPS_i consistent with each N_i and η_i bound

$$FPS_i := \{\theta \in D : N_i(\theta) \leq \eta_i, \eta_i > 0\}.$$

and its boundary

$$\partial FPS_i := \{\theta \in D : N_i(\theta) = \eta_i, \eta_i > 0\}.$$

And therefore, the FPS for all the simultaneous norms is stated as:

$$FPS := \{\bigcap_{i \in A} FPS_i\} = \{\theta \in D : \forall i \in A, N_i(\theta) \leq \eta_i, \eta_i > 0\}.$$

and its boundary

$$\partial FPS := \{\theta \in D : \exists i | N_i(\theta) = \eta_i \wedge N_j(\theta) \leq \eta_j,\ \eta_i, \eta_j > 0,\ i, j \in A\}$$

To characterize the FPS, and especially its boundary ∂FPS, a function $J(\theta)$

[7] N is the measurements number of each output and input. The interval between measurements is constant $t_i = i \cdot T_s$, being T_s the sample time.

[8] In a more general case, it would be possible to use bounds on any function.

[9] Some typical norms are absolute, infinite, or Euclidian - although any norms (see (Herrero, 2006) and its references) and even functions could be used.

is stated in such a way that its global minima constitute the ∂FPS and the FPS constitutes quasi-global minimum solutions.

$$J(\theta) := \begin{cases} \sum_B J_i \qquad if\ B(\theta) \neq \emptyset \\ \\ \min(\delta, \prod_A J_i)\ if\ B(\theta) = \emptyset \end{cases}$$

where: $B(\theta) := \{i \in A : N_i(\theta) > \eta_i\}$, and $J_i(\theta) = \left|N_i(\theta) - \eta_i\right|$.

Some of the properties of function $J(\theta)$ are:

(1) $B(\theta) = \emptyset$ when $\theta \in FPS$. $J_i(\theta) = 0$ if $\theta \in \partial FPS_i$ and $J(\theta) = 0$ if $\theta \in \partial FPS$.

(2) $J(\theta) < \delta$ when $\theta \in FPS$, therefore, it is ensured that these solutions are quasi-global minimum solutions and they will be never removed from $A(t)$ by algorithm ϵ-GA. In addition, they will not prevail over the solutions $\theta \in \partial FPS$ either, and so boundary characterization will be a priority.

With regard to the bounds selection avoiding an $FPS = \emptyset$ when a unique norm $N_1(\theta)$ is used, some authors (Walter and Piet-Lahanier, 1991) recommend selecting the bound by the $N_1(\theta)$ minimization, that is the lower bound $\eta_1^{min} = \min_\theta N_1(\theta)$ and an $FPS \neq \emptyset$ is satisfied if $\eta_1 \geq \eta_1^{min}$.

However, when several norms are simultaneously taken into account, the selection of $\eta_i \geq \eta_i^{min}$ (being $\eta_i^{min} = \min_\theta N_i(\theta)$) does not imply that $FPS \neq \emptyset$ as shown later. In this work, we propose an alternative to selecting the η_i bounds, by using the simultaneous optimization of the N_i norms, through the

following multiobjective optimization problem [10]:

$$\min_{\theta \in D} \mathbf{J}(\theta) = \mathbf{J}(\theta) = \{N_1(\theta), N_2(\theta), \ldots, N_s(\theta)\}$$

The optimization problem solution is the Pareto optimum set $\hat{\mathbf{\Theta}}_P$, or the optimum projection models for the various norms simultaneously [11].

Once the optimization problem is solved, it is possible to use the Pareto front information $\mathbf{J}(\hat{\mathbf{\Theta}}_P^*)$ for selecting the η_i bounds as shown next. Figure 2 shows the case in which two norms N_1 and N_2 of the identification error are used. It can be seen that a piece of the Pareto front $\mathbf{J}(\hat{\mathbf{\Theta}}_P)$, that depends on the selected bounds η_1 and η_2 and corresponds to the restricted projection optimum models $\mathbf{J}(\hat{\mathbf{\Theta}}_{Pr})$ stands out in the figure.

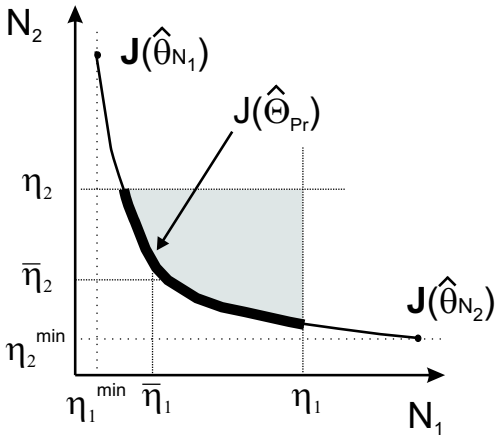

Figure 2. The minimum bounds η_1^{min} and η_2^{min} and $\mathbf{J}(\hat{\mathbf{\Theta}}_{Pr})$ which depend on the selected bounds $\eta_1 > \eta_1^{min}$ and $\eta_2 > \eta_2^{min}$.

[10] The computational burden is reduced as only a single multiobjective optimization is made, instead of s independent optimizations of the corresponding N_i $(i \in s)$.

[11] The algorithm ϵ-MOGA (Herrero, Blasco, Martínez and Ramos, 2005) is used to determine $\hat{\mathbf{\Theta}}_P$. The algorithm solution consists of a finite set $\hat{\mathbf{\Theta}}_P^*$ of optimum models distributed along the Pareto front. Since $\hat{\mathbf{\Theta}}_P^*$ contains the Pareto front ends, it also contains the independent projection estimations $\hat{\theta}_{N_i} = \arg\min_{\theta \in FPS} N_i$.

Therefore, it is sufficient to select η_i in such a way $\hat{\mathbf{\Theta}}_{Pr} \neq \emptyset$ to ensure that $FPS \neq \emptyset$, since $\hat{\mathbf{\Theta}}_{Pr} \subset FPS$. The figure shows that the selected bounds η_1 and η_2 ($\eta_1 > \eta_1^{min}$ and $\eta_2 > \eta_2^{min}$) achieve $\hat{\mathbf{\Theta}}_{Pr} \neq \emptyset$. The dark zone (bounded by the bounds η_1, η_2 and the Pareto front itself) contains $\mathbf{J}(FPS)$ in the space (N_1, N_2). If bounds $\bar{\eta}_1$ and $\bar{\eta}_2$ ($\bar{\eta}_1 > \eta_1^{min}$ and $\bar{\eta}_2 > \eta_2^{min}$) had been used, $\hat{\mathbf{\Theta}}_{Pr} = \emptyset$ and therefore $FPS = \emptyset$ there would have been no dark zone. So it is proved that $\bar{\eta}_i > \eta_i^{min}$ is an insufficient condition for $FPS \neq \emptyset$.

3.1 FPS validation

Once the feasible parameter set FPS_{ide} is determined via RI, using the experimental data $\Omega_{ide} = \{\mathbf{Y}_{ide}, \mathbf{U}_{ide}\}$, the s norms N_i and their bounds η_i must be validated by using different experimental data $\Omega_{val} = \{\mathbf{Y}_{val}, \mathbf{U}_{val}\}$.

One method of validation consists of checking whether the FPS_{ide} contains models that are consistent with new data Ω_{val}. That means that the FPS obtained by process identification with data $\Omega = \{\Omega_{ide}, \Omega_{val}\}$ would be $FPS \neq \emptyset$. In figure 3 two cases are shown. In the first case, there are models in the FPS_{ide} that also belong to the FPS_{val} (set consistent with Ω_{val} and with the same s norms N_i and bounds η_i used for FPS_{ide}) and, therefore, the FPS_{ide} is validated; and in the second case, this does not occur and so the FPS_{ide} is invalidated.

If the FPS_{ide} is validated, the final FPS will be $FPS = FPS_{ide} \bigcap FPS_{val}$. It is not necessary to obtain the FPS_{val}, but it is necessary to maintain in the FPS those models from FPS_{ide} which are consistent with the data Ω_{val}. Since the finite set FPS_{ide}^{*} is available, obtaining the FPS^{*} is easy, because

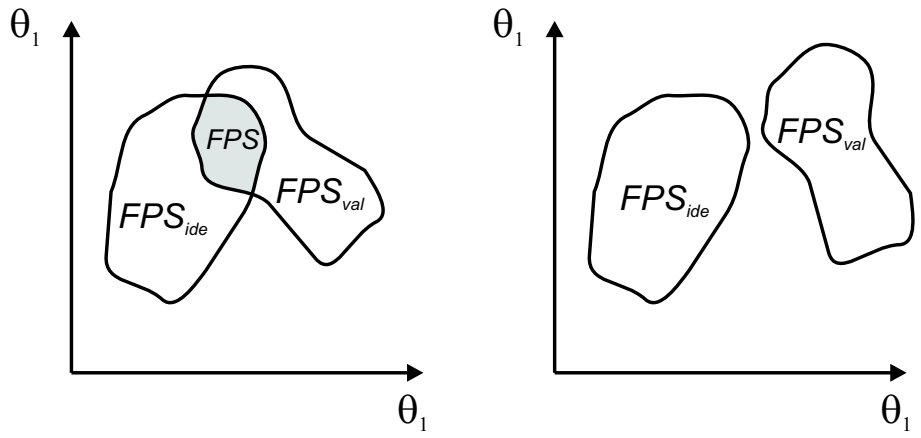

Figure 3. Validation process. On the left, the FPS_{ide} is validated, since $FPS \neq \emptyset$. On the right, the FPS_{ide} is invalidated since $FPS = \emptyset$.

it is only necessary to simulate the models $\theta \in FPS^*_{ide}$ (using Ω_{val}) and to choose those which satisfy $N_i(\theta) \leq \eta_i \; \forall i \in A$.

If the FPS_{ide} is invalidated, several actions could be considered: increase some, or all, of the η_i bounds until the FPS_{ide} can be validated with data Ω_{val}; or to modify the model (for instance, by adding part of the non-modelled dynamics) until the FPS_{ide} is validated. In this second action, it is not necessary to increase the η_i bounds and so model prediction performance is not deteriorated - as occurs with the first action. However, the model in the second case is more complex.

4 Greenhouse model

For some time now, agricultural engineers have been working to perfect models of the physical and physiological processes that take place inside greenhouses based on mass and energy balances, including the biological behaviour of plants. In (Stanghellini and de Jong, 1995) there is a groundbreaking study on the description of a model of the humidity in a greenhouse that is based on

obtaining a first principles non-linear model of the humidity by defining the balance of condensation, ventilation, and transpiration flows. In this last case, the Penman-Monteith equation (Monteith, 1973) is used to incorporate the saturation and radiation deficit measurements so they can be evaluated. This model is still utilised today to design the ventilation systems in greenhouses (Seginer, 2002). The humidity model is complemented by energetic balance models at different levels. Again, a first principles equation is constructed to include the balance of thermal flows associated with the ventilation, convection, conduction, and latent heat, due to plant transpiration (Jolliet and Bailey, 1992; Baille, Baille and Delmon, 1994) that define temperature evolution. Equations can be defined for the temperature evolution in each greenhouse, depending on their different volumes and floor areas, and the interactions among them. The model can vary in its complexity depending on the number of volumes selected, which give rise to a higher, or lower, number of differential equations (Blasco, 1999; Rodríguez, 2002).

In this study, the greenhouse is considered to be a volume of air that is delimited by the walls, the roof, and the floor, so establishing two subsystems: namely, the volume of air and the floor, this latter acting as a thermal mass (Albright, Seginer, Marsh, and Oko, 1985). Some hypotheses are considered (Rodríguez, 2002): the walls and the roof are homogeneous material with insignificant heat capacity and constant optic properties; the crop density is homogeneous and its heat capacity is insignificant too; the air is homogeneous and is considered inert to radiation process; and the approximation presented in (Boulard and Draoui, 1995) is used to calculate the renewal air flow.

The state variables that describe the climatic behaviour are temperature $\hat{T}_i$ ($\hat{.}$ is used for the model output variables) and humidity $\hat{HR}_i$ (or absolute

humidity H_i) in the air and floor temperature T_m (called the thermal mass temperature).

The water mass balance and air energy balance establish the first two equations of state, and the third is set by the energy balance over thermal mass.

$$\rho v_i \frac{dH_i}{dt} = F_v + C_{sat}(E + fog), \tag{8}$$

$$v_i \rho c_p \frac{d\hat{T}_i}{dt} = Q_s - Q_{cc} + Q_m - Q_v - C_{sat}(Q_e + Q_n) + W. \tag{9}$$

$$A_i C_m \frac{dT_m}{dt} = Q_{sm} - Q_m - Q_f. \tag{10}$$

where: the inside temperature $\hat{T}_i$ and the temperature of the thermal mass T_m are in ^oC; the absolute inside humidity H_i is in Kg_{H_2O}/Kg_{air}; the volume of the greenhouse v_i is given in m^3 and the area A_i in m^2; the density of the air ρ is in Kg_{air}/m^3; specific heat of the air c_p is in $JKg^{-1}\ ^oC^{-1}$; the air saturation coefficient C_{sat} is dimensionless and the heat capacity of the thermal mass C_m is given in $Jm^{-2}\ ^oC^{-1}$.

The flows in the mass balance are: (all in Kg_{H_2O}/s): F_v; renovation flow due to the window opening; E, crop evapotranspiration, which is estimated from the Penman-Monteith equation (Monteith, 1973) and has important non-linearities; and fog, which is the water produced by the fog system.

The energy balance terms are (all in W): Q_s, solar energy supplied to the air; Q_{cc}, energy exchange due to conduction and convection; Q_m, energy exchange with the thermal mass; Q_e, energy loss due to crop evapotranspiration; Q_n, energy loss due to fogging; Q_v, energy exchange due to ventilation and W, energy from heating system.

The energy balance terms are (all in W): Q_m, energy exchanges between the

thermal mass and the inside air; Q_{sm}, energy stored by the thermal mass during the day and Q_f, losses into the ground.

The output variables are: inside humidity $\hat{H}R_i$ in % and inside temperature $\hat{T}_i$ in ^oC. The input variables that can be manipulated are: window opening control $MV_\alpha \in [0, 100]\%$; heating control $MV_w \in [0, 100]\%$ and fog control $MV_{fog} \in [0, 100]\%$. Figure 4 shows an input/output model diagram.

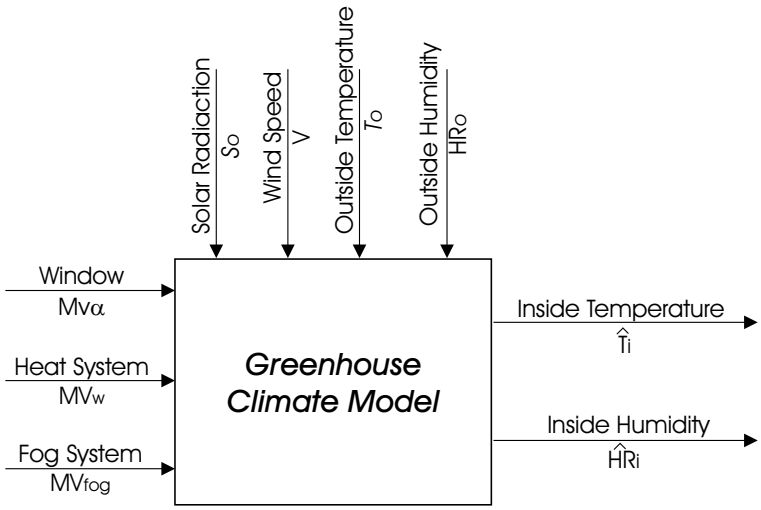

Figure 4. Greenhouse climatic model.

Measurable disturbances are: solar radiation S_o in $W \cdot m^{-2}$; outside temperature T_o in ^oC; outside humidity HR_o in % and wind speed V in m/s.

As can be seen in Appendix 7.1, the model has many parameters. Some are easy to determine, for example, the volume and the area of the greenhouse, but others, such as the maximum stomatal conductance are not so simple. The complexity of the model and the large number of unknown parameters, together with the fact that some vary over time, make them difficult to handle.

5 Greenhouse Robust Identification

5.1 Planning the experiments

The operating conditions of a greenhouse are potentially altered by the effects of disturbances, mainly due to solar radiation and outside temperature. These disturbances follow a typical behaviour that is repeated daily and which depends largely on the time of year. Thus, it is impossible to give a single set of parameters $\hat{\theta}$ which enables the reproduction of greenhouse behaviour throughout the year. In Mediterranean areas, greenhouse control in summer is a challenging problem. This model will therefore be adjusted to cover the dynamics found in the summer period (day and night). It is worth noting that at this time of year heating is not used, and so this actuator is not taken into account.

To simplify identification, some authors (Rodríguez, Yebra, Berenguel and Dormido, 2002) distinguish between day and night, and propose particular conditions to independently identify some of the model parameters. This work does not use these simplifications and proposes an identification of the parameter model and setting uncertainties using daily data (no requirement for special experiments) that will facilitate practical application.

The experiments will last for a multiple 24-hour period. The more days used, the more accurately the model will represent the period. A large number of days, however, makes the simulations costly to perform and the time required to fit the model increases considerably. This approach tries to simulate a real application where a model could be adjusted with daily data in a reasonable

time at the beginning of the summer and subsequently used during all of the summer for control. This is why, in this case, and as a compromise, two (non-consecutive) days were chosen. This may seem too little data for identification, but remember the RI approach is deterministic and it is not necessary to establish statistical properties of the IE (which would require more data).

For the identification task, data from the 11th and 15th June 2002 was used [12] (see figure 11). Although this data is restricted to two specific days, it will be shown that it is possible to obtain an FPS validated with data for the days of 20th June, 28th July, 22nd August and 8th September 2002 - with very different conditions (see figure 12).

5.2 Norms and bounds selection

Before selecting norms and bounds to use in RI, the following aspects need to be dealt with: the model adaptation; selection of the parameters to be identified; the procedure for establishing the initial conditions; and the optimality criteria to be applied.

With regard to the model adaptation, in the particular case of the greenhouse climatic model (figure 4), the state equations (8), (9) and (10) are adapted directly to the generic equation (6).

In relation to the parameter selection, for the case of hydroponic cultivation of roses in a greenhouse, the candidate set of parameters to be estimated (θ) is associated with the specific growing of rosebushes and with parameters that

[12] The sampling period was 15 seconds, which is more than enough to capture the dynamics of the processes taking place in the greenhouse.

are associated with different heat transfer constants and reference temperatures inside the greenhouse. The meaning of each parameter to be identified, together with its adjustment range, can be consulted in the Notation section in the appendix. The physical sense of the parameters (which permits an analytical approximation of values) together with previous identification works (Martínez, Blasco, Herrero, Ramos and Sanchis, 2005) have enabled us to suggest these approximate ranges (even taking into account the simplifications made in the model), and as a result, the search area is drastically reduced. Thus, adapting the generic problem in state variables to the greenhouse model results in:

$$\theta = [gws_{max}\ \ gws_{min}\ \ k\ \ L\ \ gwb\ \ \tau\ \ a\ \ G_o\ \ Ac\ \ C_m\ \ h_m\ \ T_{ref}\ \ \alpha_m\ \ k_a\ \ fog_{max}]^T,$$

$$\mathbf{u}(t) = [MV_\alpha\ MV_{fog}\ S_o\ T_o\ HR_o\ V]^T, \hat{\mathbf{y}}(t) = \left[\hat{T}_i\ \hat{HR}_i\right]^T, \mathbf{x}(t) = \left[H_i\ \hat{T}_i\ T_m\right]^T.$$

The states will be initialised using real variable measurements. The first state variable H_i can therefore be initialised directly from the value of the outputs $T_i(0)$ and $HR_i(0)$ in the initial time, as indicated in Appendix 7.2 (equation (15) & (16)). The second state variable $\hat{T}_i$ is at the same time an output variable, and it can therefore be initialised with the value of this output in the initial moment $T_i(0)$. Initialisation of the third state variable T_m is not so straightforward because there is no sensor to measure it. The initial value of $T_m(0)$ will be estimated using information from inputs and outputs in the initial moment and the equation (9) for the energy balance in the air. Since the simulations are started at night (and hence $S_o = 0$) and without activating the fogging system, the equation would be as follows:

$$v_i \rho c_p \frac{dT_i(0)}{dt} = -Q_{cc}(0) + Q_m(0) - Q_e(0) - Q_v(0).$$

which, on expansion, would give:

$$v_i \rho c_p \frac{dT_i(0)}{dt} = -A_i A_c (T_i(0) - T_o(0)) + A_i h_m (T_m(0) - T_i(0)) - \lambda E(0) \\ - \rho c_p A V(0)(a\alpha + G_o)(T_i(0) - T_o(0)).$$

It can be assumed that $\frac{d\hat{T}_i(0)}{dt} = 0$ since it varies very little at night (for the summer days $dT_i(0)/dt \approx 0.1 \cdot 10^{-3}\ Cs^{-1}$ was used in the identification), so that $T_m(0)$ was obtained in the following way:

$$T_m(0) = \frac{1}{A_i h_m}\Big(A_i A_c (T_i(0) - T_o(0)) + \lambda E(0) \\ + \rho c_p A V(0)(a\alpha + G_o)(T_i(0) - T_o(0)) \Big) + T_i(0),$$

where:

$$E(0) = \frac{A_i 2L\rho\, c_p\, D_i(0)\, gwb}{\left(\Delta + \gamma\left(1 + \frac{gwb}{gws_{min}}\right)\right)\lambda}.$$

Four IE norms will be taken into account simultaneously. ∞-norm N_1 and absolute norm N_3 applied to inside temperature and ∞-norm N_2 and absolute norm N_4 applied to inside humidity. In this way, integral error and sample error will be bounded throughout the data experiment [13].

$$N_1 = \|\mathbf{e}_1(\theta)\|_1,\ N_2 = \|\mathbf{e}_2(\theta)\|_1,\ N_3 = \|\mathbf{e}_1(\theta)\|_\infty,\ N_4 = \|\mathbf{e}_2(\theta)\|_\infty. \qquad (11)$$

[13] The selected norms influence the FPS (Bai, Nagpal and Tempo, 1996), however their relation is difficult to discover and more so when non-linear models are used; and so the norms have been selected in such a way that they present a practical meaning related to the performance prediction for the IE.

where $e_1(t_j,\theta) = T_i(t_j) - \hat{T}_i(t_j,\theta)$, $e_2(t_j,\theta) = (HR_i(t_j) - \hat{H}R_i(t_j,\theta))k_j$ and:

$$k_j = \begin{cases} -0.02 * \hat{H}R_i(t_j) + 2.2 & if\ \hat{H}R_i(t_j) \in [60 \ldots 100]\% \\ \\ 1 & if\quad \hat{H}R_i(t_j) \in [0 \ldots 60[\% \end{cases}.$$

The purpose behind using k_j is to weigh any errors that are produced for higher levels of humidity, so giving them a lower relative importance. The reason for this is related with the commercial humidity sensor used, since its accuracy drops notably for these values (due to condensation that is usually produced on the sensor because of the lack of ventilation). Figure 5 shows the relationship between K_j and $\hat{H}R_i(t_j)$. It can be observed that the errors produced for relative humidity values of around 100 % are weighted by 0.2; that is to say, they have a lower relative importance than those that occur for humidity values of 60 %.

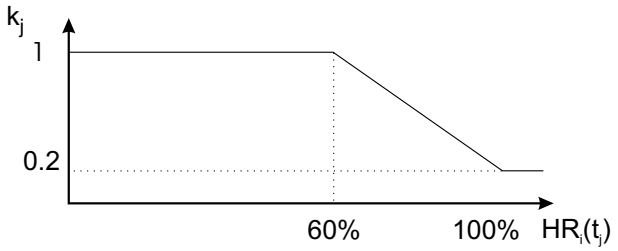

Figure 5. $k_j = f(\hat{H}R_i(t_j))$. $\hat{H}R_i(t_j)$ inside relative humidity at sample t_j.

To select the norm bounds η_1, η_2, η_3 and η_4 the Pareto front information from the following multiobjective optimization problem is considered:

$$\min_{\theta \in D} \mathbf{J}(\theta) = \{N_1, N_2, N_3, N_4\}. \tag{12}$$

Figure 6 shows the Pareto front corresponding to the projection optimum models $\hat{\mathbf{\Theta}}_P^*$.

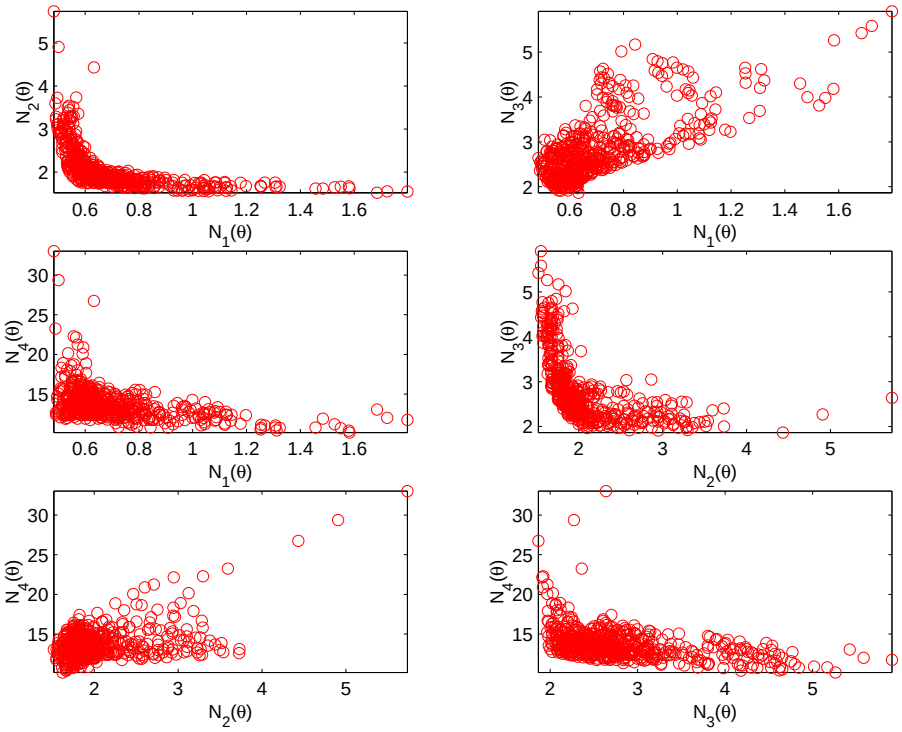

Figure 6. Projections of the Pareto front $\mathbf{J}(\hat{\mathbf{\Theta}}_P^*)$ on different planes $(N_1(\theta), N_2(\theta))$, $(N_1(\theta), N_3(\theta))$, $(N_1(\theta), N_4(\theta))$, $(N_2(\theta), N_3(\theta))$, $(N_2(\theta), N_4(\theta))$ and $(N_3(\theta), N_4(\theta))$.

From Pareto front analysis it is possible to obtain the minima:

$$\eta_1^{min} = \min N_1(\theta) = 0.483^o C, \ \eta_2^{min} = \min N_2(\theta) = 1.51\%,$$

$$\eta_3^{min} = \min N_3(\theta) = 1.86^o C, \ \eta_4^{min} = \min N_4(\theta) = 10.13\%.$$

and therefore the ideal point $\mathbf{J}^{ideal}$ will be

$$\mathbf{J}^{ideal} = \{\eta_1^{min}, \eta_2^{min}, \eta_3^{min}, \eta_4^{min}\} = \{0.483, 1.51, 1.86, 10.13\}.$$

An ideal model would be determined as:

$$\theta^{ideal} = \arg\min_{\theta \in \hat{\mathbf{\Theta}}_P^*} ||\mathbf{J}(\theta) - \mathbf{J}^{ideal}||_2 = [0.010078, 0.002865, 0.41594, 0.72374, 0.016825, 0.30016, 0.0011995, 0.00025871, 19.519, 1.8596e^5, 9.4531, 18.732, 0.012533, 1.4839, 0.0019266], \quad (13)$$

$$\mathbf{J}(\theta^{ideal}) = \{0.623, 2.16, 2.12, 12.74\}. \quad (14)$$

Bounds $\eta_1 = 0.8$, $\eta_2 = 3$, $\eta_3 = 3$ and $\eta_4 = 20$ are selected from the Pareto front analysis in order to hold the FPS_{ide} model prediction errors not greater than 0.8^oC and 3% and their average values not greater than 3^oC and 20%. So $\hat{\Theta}_{Pr} \neq \emptyset$ and therefore $FPS \neq \emptyset$ [14].

5.3 Robust identification

There are some parameters with low sensitivity, and so the FPS_{ide} will only be associated with some of them. Therefore, to select these parameters a sensitivity analysis will be made as follows. Taking θ^{ideal} as the reference model, each parameter is modified along its search space and the variation of each norm is evaluated. Table 1 shows the sensitivity analysis results where it is possible to check that gws_{max}, gws_{min}, k, G_o, C_m, T_{ref}, α_m and k_a parameters have lower sensitivity than the other parameters. Consequently, their value will be matched with the correspondent parameter value of the ideal model, and hence their uncertainty will not be determined. Thus, the search space of FPS_{ide} and the number of models that FPS_{ide} it contains will be reduced.

The FPS^*_{ide} is determined next by $\epsilon - GA$ with the following parameters:

- search space D is associated with the limits of the following parameters $\theta = [L, gwb, \tau, a, A_c, h_m, fog_{max}]$ [15] which can be checked in appendix 7.1.

[14] With linear models minimum bound η_1^{min}, η_2^{min}, η_3^{min}, η_4^{min} will be greater and probably with $\eta_1 = 0.8$, $\eta_2 = 3$, $\eta_3 = 3$ and $\eta_4 = 20$ the $FPS = \emptyset$. Therefore, a non-linear model is necessary for an adequate approximation with these bounds.

[15] Some of these parameters are time variable. For example: the leaves area index L (related to crop state); transmission coefficient of the greenhouse τ (related to cover dirtiness); maximum water rate of fog system fog_{max} (since lime modifies fog

- $t_{max} = 40000$ and $\epsilon = [0.19, 0.0098, 0.08, 0.00099, 2.8, 5.8, 0.00398]$ so the grid contains 10 divisions per dimension for L, τ, a and A_c (because they have high sensitivity) and five for gwb, h_m and fog_{max}.
- $Nind_P = 100$, $Nind_G = 4$, $P_{c/m} = 0.1$, $d_{ini} = 0.25$, $d_{fin} = \beta_{fin} = 0.1$ and $\beta_{ini} = 10$. $\delta(t)$ is tuned as $\delta(t) = \delta'(t) \cdot \bar{J}$, in order to be useful for other optimization problems, where $\bar{J}$ is the average J for all the individuals inserted in the population $P(t)$ during the optimization process. So an average estimation of function J is obtained and δ is related to the optimization problem [16] . $\delta'(t)$ is determined by:

$$\delta'(t) = \frac{\delta_{ini}}{\sqrt{1 + \left(\left(\frac{\delta_{ini}}{\delta_{fin}}\right)^2 - 1\right) \frac{t}{(t_{max}-1)}}}, \quad \delta_{ini} = 0.1, \delta_{fin} = 0.01.$$

Figure 7 shows the ϵ-GA optimization process result, i.e. FPS^*_{ide}. The FPS_{ide} has been characterized by 4208 models and the average $J(\partial FPS^*_{ide})$ is 0.0019, which shows the good algorithmic convergence (the ideal average $J(\partial FPS^*_{ide})$ would be 0). The evaluation number of $J(\theta)$ function was 160100, that is, approximately the eighth part of what would have been necessary if $J(\theta)$ had been evaluated in each box of the grid [17] (exhaustive search).

Figure 8 shows the Y_{ide} data, and the envelope generated by the FPS^*_{ide}. It can be seen that the envelope captures the real data $Y_{ide}(t)$.

Figures 9 and 10 show the $Y_{val1} \ldots Y_{val4}$ data with the envelope from FPS_{ide}.

system efficacy); etc.

[16] Only those values inserted in $P(t)$ lower than $\bar{J}$ are taken into account to ensure that $\delta(t)$ never increases.

[17] To evaluate 160,100 times the $J(\theta)$ function took four hours, whereas approximately 32 hours would have been necessary with an exhaustive search and the FPS_{ide} characterization would have been worse.

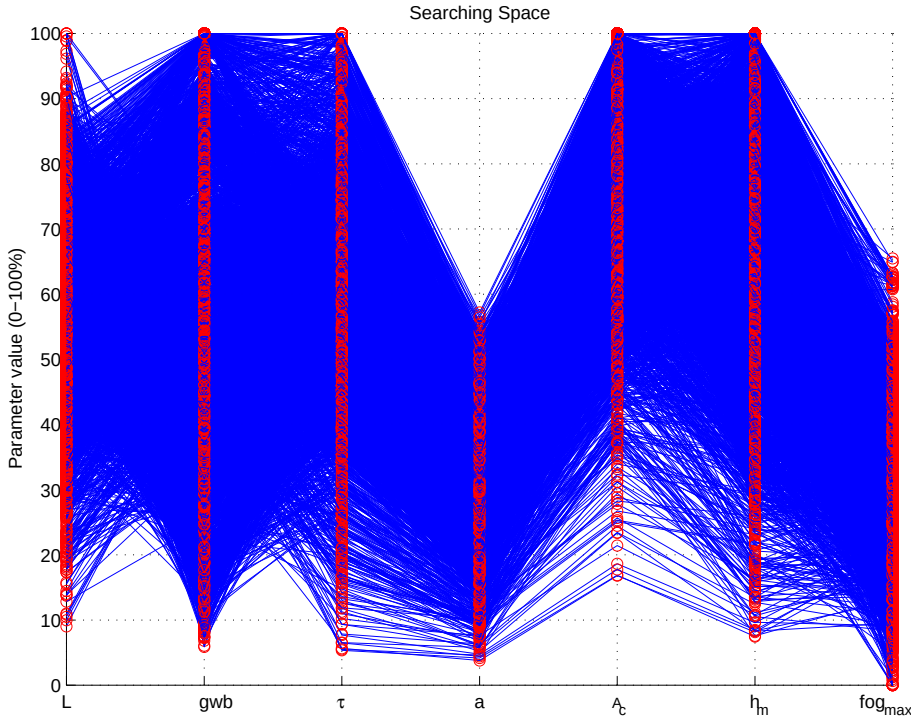

Figure 7. Each line represents a model of FPS^{*}_{ide} inside the search space. The horizontal axis represents the seven parameters of each model, whereas the vertical axis shows the parameter values in % with respect to the limits of their search space. There are 16 models consistent with Ω_{val1}, five with Ω_{val2}, 51 with Ω_{val3} and with Ω_{val4}, so FPS_{ide} is validated.

6 Conclusions

A methodology, based on a specific genetic algorithm $\epsilon-$GA, has been developed to find the feasible parameter set (FPS) of a non-linear model under parametric uncertainty. That robust identification problem is formulated by assuming, simultaneously, the existence of several bounds in identification error. The algorithm presents the following features:

- Assuming parametric uncertainty, all kinds of processes can be identified if

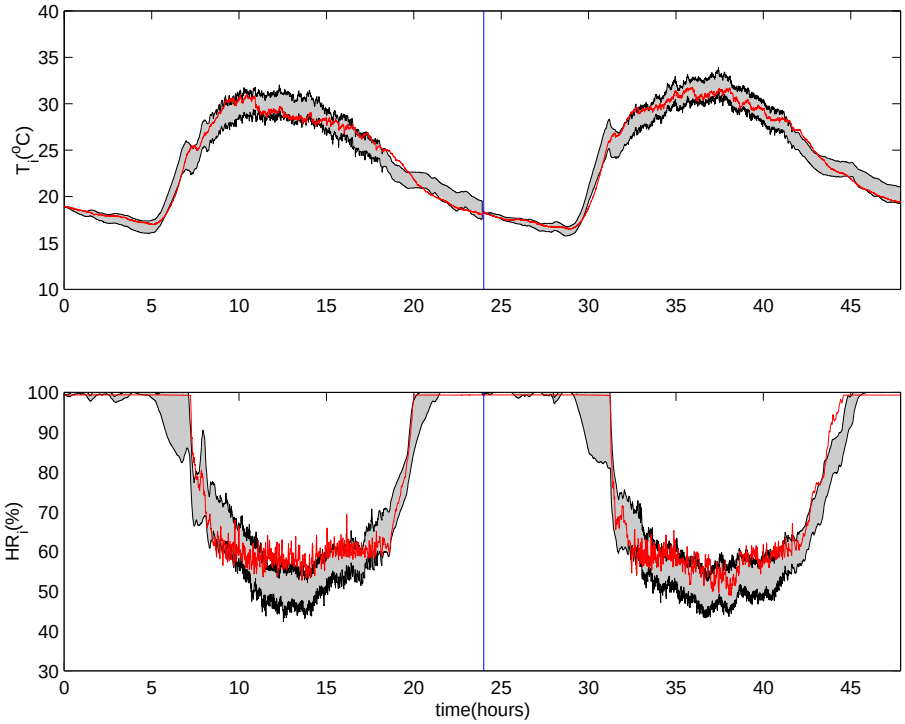

Figure 8. $Y_{ide}(t)$ and the FPS^*_{ide} models envelope.

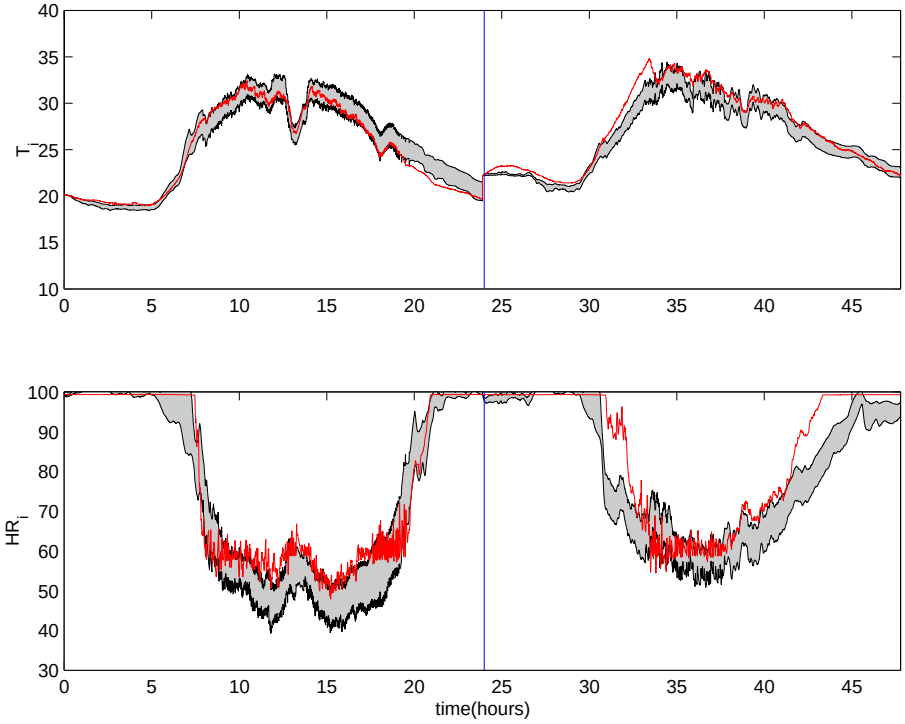

Figure 9. $Y_{val1}(t)$, $Y_{val2}(t)$ and the FPS^*_{ide} models envelope.

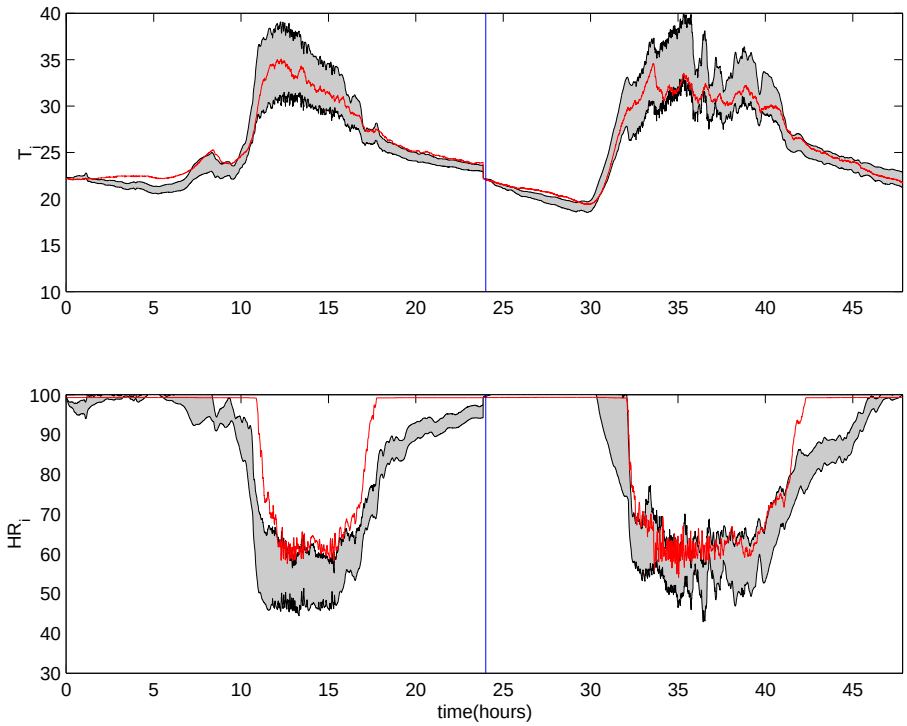

Figure 10. $Y_{val3}(t)$, $Y_{val4}(t)$ and the FPS^*_{ide} models envelope.

their outputs can be calculated by model simulation. Differentiability with respect to the unknown parameters is unnecessary.

- Because more than one norm is taken into account at the same time, the computational cost is reduced as various FPS_i intersections are implicitly performed.
- Non-convex even disjoint $C(FPS)$ can be calculated.
- Since FPS is approximated by neither orthotopes nor ellipsoids, a non-conservatism is provided.

An intuitive procedure to help to select the bounds η_i associated with $N_i(\theta)$ norms so that $FPS \neq \emptyset$ has been presented. This procedure uses the information that produces the Pareto front obtained when the $N_i(\theta)$ norms are minimized simultaneously in a multiobjective optimization problem.

The principal advantages of the RI methodology presented are flexibility and power.These advantages have been demonstrated through the RI of the non-linear greenhouse climate model presented with real data from a summer in the Mediterranean area. This methodology has enabled the registration of the FPS associated with seven unknown model parameters when four norms are applied simultaneously on inside temperature and humidity. To solve this RI problem with other methodologies implies a more difficult task as a consequence of the model non-linearities and norm chosen.

Future work will use a model of the FPS in a predictive control algorithm where FPS will produce an envelope of future prediction (similar to those of figures 8, 9 and 10). The controller objective will be to keep both temperature and humidity envelopes inside the desired range and reduce energy and water consumption as in (Blasco, Martínez. Herrero, Ramos and Sanchis, 2007).

Acknowledgments

Partially supported by MEC (Spanish government) and FEDER funds: projects DPI2005-07835 and DPI2004-8383-C03-02

7 Appendix

7.1 Notation

Range of possible values are indicated for identifiable parameters. Exact values are indicated for constant or known parameters.

A: Window area, 130 m^2

A_c: Loss coefficient of conduction and convection, [2, 20]

A_i: Greenhouse surface area, 240 m^2

a: Constant for renewal volumetric flow, [0.0005, 0.01]

C_m: Thermal mass heat capacity, [100000, 300000] $J\ ^oC^{-1}\ m^{-2}$

c_p: Air heat capacity, 1003 $J\ Kg^{-1}\ ^oC^{-1}$

C_{sat}: Air saturation coefficient, dimensionless

D_i: Air water vapour deficit, KPa

E: Crop evapotranspiration, Kg_{H_2O}/s

F_v: Water rate in the air renewal flow, Kg_{H_2O}/s

fog: Water rate of fog system, Kg_{H_2O}/s

fog_{max}: Maximum water rate of fog system, [0.001, 0.005] Kg_{H_2O}/s

F_v: Water rate in the air renewal flow, Kg_{H_2O}/s

G: Renewal air flow, m^3/s

G_o: Losses of renewal air flow, [0.0005, 0.01]

gwb: Boundary-layer conductance, [0.001, 0.05] m/s

gws: Stomatal conductance, m/s

gws_{max}: Maximum stomatal conductance, [0.01, 0.03] m/s

gws_{min}: Minimum stomatal conductance, [0.0001, 0.005] m/s

h_m: Conductivity coefficient between air and thermal mass, [1,20] $W\ m^{-1}\ ^o\ K^{-1}$

H_i: Inside absolute humidity, Kg_{H_2O}/Kg_{air}

H_o: Outside absolute humidity, Kg_{H_2O}/Kg_{air}

H_{sat}: Absolute saturation humidity, Kg_{H_2O}/Kg_{air}

$\hat{H}R_i$: Inside relative humidity, %

HR_o: Outside relative humidity, %

k: Extinguishing coefficient of radiation, [0.1, 0.7]

k_a: Conductivity coefficient between thermal mass and ground, [0.5, 10]

$W\ m^{-1}\ ^{o}\ K^{-1}$

L: Leaves area index, [0.5, 2] $m^2_{leaves}/m^2_{ground}$

MV_{α}: Windows opening manipulated variable, %

MV_{fog}: Fog system manipulated variable, %

MV_W: Heating system manipulated variable, %

P: Atmospheric pressure, 98.1 KPa

$psat$: Saturation pressure, KPa

Q_{cc}: Energy exchange by conduction and convection phenomena, W

Q_e: Energy loss due to crop evapotranspiration, W

Q_f: Energy loss through ground, W

Q_m: Energy exchange with thermal mass, W

Q_n: Energy loss by nebulization, W

Q_s: Solar energy supplied to air volume, W

Q_{sm}: Energy stored by the thermal mass during the day, W

Q_v: Energy exchange due to window ventilation, W

Rn: Solar radiation absorbed by the crop, W/m^2

S_o: Solar radiation, W/m^2

$\hat{T}_i$: Inside temperature, ^oC

T_m: Thermal mass temperature, ^oC

T_o: Outside temperature, ^oC

T_{ref}: Ground temperature at reference depth, [10, 20] ^oC

V: Wind speed, m/s

v_i: Greenhouse volume, 850 m^3

W: Energy from heating system, W

W_{max}: Maximum power of heating system, 5000 W

z_{ref}: Reference depth, 6 m

α: Opening window angle, ^{o}

α_m: Rate of absorbed heat by thermal mass, [0.01, 0.3]

α_{max}: Maximum window angle, 12^o

Δ: Slope of water vapour saturation, $KPa/^oC$

γ: Psycrometric constant, 0.066 $KPa/^oC$

λ: Latent heat of vaporization, J/Kg

ρ: Air density, 1.25 Kg_{air}/m^3

τ: Transmission coefficient of the greenhouse, [0.3, 0.9]

7.2 Complementary equations

Opening window angle: $\alpha = \frac{MV_\alpha}{100}\alpha_{max}$.

Water rate of fog system: $fog = \frac{MV_{fog}}{100}fog_{max}$.

Energy from heating system: $W = \frac{MV_W}{100}W_{max}$.

Water rate in the air renewal flow: $F_v = \rho G(H_o - H_i)$.

Renewal air flow (Boulard and Draoui, 1995): $G = AV(a\alpha + G_o)$.

Air saturation coefficient:

$$C_{sat} = \begin{cases} 1 & H_i < H_{sat} \\ \\ 0 & H_i = H_{sat} \end{cases}.$$

Absolute to relative humidity conversion [18] :

$$HR = \begin{cases} 100 \;\; HR > 100 \\ \\ HR \; HR \leq 100 \end{cases},$$

$$HR = \frac{100H \cdot P}{0.611 psat(T)}, \tag{15}$$

$$p_{sat}(T) = 0.61 \left[1 + 1.414 \sin(5.82e^{-3}T)\right]^{8.827}. \tag{16}$$

Crop evapotranspiration (Monteith, 1973):

$$E = \frac{A_i(\Delta Rn + 2L\rho\, c_p\, D_i\, gwb)}{\left[\Delta + \gamma\left(1 + \frac{gwb}{gws}\right)\right]\lambda},$$

$$\Delta = p_{sat}(\hat{T}_i + 0.5) - p_{sat}(\hat{T}_i - 0.5), \quad Rn = (1 - e^{kL})\tau So$$

$$D_i = p_{sat}(\hat{T}_i)\left[1 - \frac{\hat{H}R_i}{100}\right], \quad \lambda = (3.1468 - 0.002365(\hat{T}_i + 273)10^6$$

$$gws = gws_{min} + (gws_{max} - gws_{min}) \cdot \left[1 - exp\left(-\frac{\tau So}{160}\right)\right] g_D,$$

[18] Depending on different cases, (T,HR,H) corresponds to the inside ($\hat{T}_i, \hat{H}R_i, H_i$) or outside ($T_o, HR_o, H_o$) of the greenhouse. It also enables calculation of the saturation absolute humidity H_{sat} corresponding to $HR = 100\%$.

$$g_D = \begin{cases} \frac{0.39}{0.029+D_i} & D_i \geq 0.361 \\ 1 & D_i < 0.361 \end{cases}.$$

Solar energy supplied to air volume: $Q_s = A_i \tau So$.

Energy exchange by conduction and convection: $Q_{cc} = A_i A_c (\hat{T}_i - T_o)$.

Energy loss due to crop evapotranspiration: $Q_e = \lambda E$.

Energy exchange due to window ventilation: $Q_v = \rho c_p G (\hat{T}_i - T_o)$.

Energy loss by nebulization: $Q_n = \lambda fog$.

Energy exchange between thermal mass and inside air: $Q_m = A_i h_m (T_m - \hat{T}_i)$.

Energy stored by the thermal mass during the day: $Q_{sm} = \alpha_m Q_s$.

Energy loss through ground: $Q_f = A_i k_a \left(\frac{T_m - T_{ref}}{z_{ref}}\right)$.

7.3 Identification and validation data

Figure 11 shows the input (manipulations and perturbations) data $U_{ide}(t)$ which have been used in the identification process. This data together with $Y_{ide}(t)$ (see figure 8) constitutes the $\Omega_{ide} = \{Y_{ide}(t), U_{ide}(t)\}$ identification data.

Figure 12 shows the input data $U_{ide1}(t)$, $U_{ide2}(t)$, $U_{ide3}(t)$ and $U_{ide4}(t)$ which have been used in the validation process. These data together with $Y_{val1}(t)$, $Y_{val2}(t)$, $Y_{val3}(t)$ and $Y_{val4}(t)$ (see figures 9 and 10) constitutes the Ω_{val1}, Ω_{val2}, Ω_{val3} and Ω_{val4} validation data.

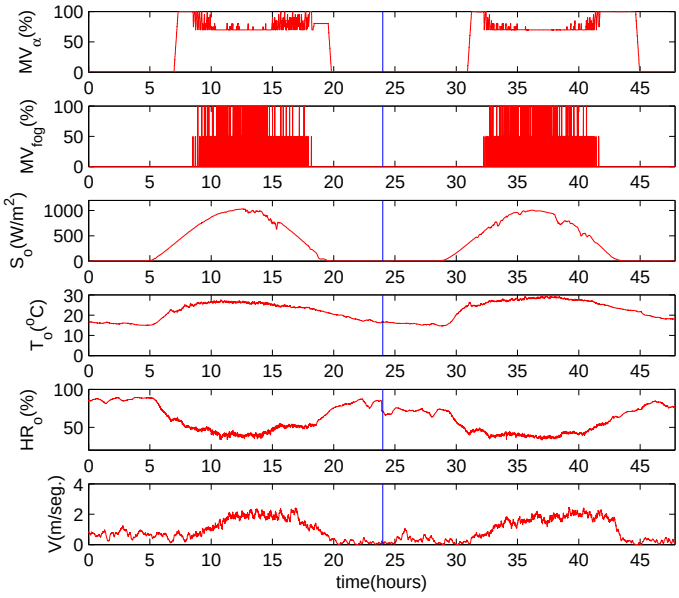

Figure 11. $U_{ide}(t)$ identification data corresponding to data collected on 11th (left) and 15th (right) June 2002.

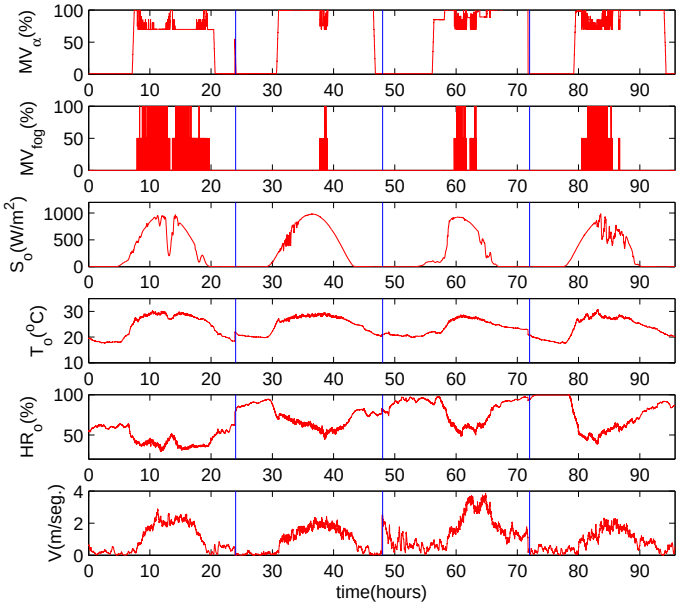

Figure 12. $U_{val1}(t)$, $U_{val2}(t)$, $U_{val3}(t)$, $U_{val4}(t)$ validation data corresponding to data collected on 20th June, 28th July, 22nd August and 8th September 2002 (from left to right).

References

Albright D, Seginer I, Marsh L, Oko A. In situ thermal calibration of unventilated greenhouses. Journal of Agricultural Engineering Research 1985; 31: 265–281.

Bäck T, Schwefel H.P. Evolution Strategies I: variants and their computational implementation. Genetic Algorithms in Engineering and Computer Science, John Wiley & Sons Ltd, 1995; chapter 6: 111–126.

Bai E, Nagpal K, Tempo R. Bounded-error parameter estimation: noise models and recursive algorithms. Automatica 1996; 32(7): 985–999.

Baille M, Baille A, Delmon D. Microclimate and transpiration of a greenhouse rose crop. Agric. Forest Meteor 1994; 71: 83–87.

Belforte G, Bona B, Cerone V. Parameter estimation algorithms for a set-membership description of uncertainty. Automatica 1990; 26(5): 887–898.

Blasco X, Martínez M, Herrero JM, Ramos C, Sanchis J. Model-based predictive control of greenhouse climate for reducing energy and water consumption. Computers and Electronics in Agriculture 2007; 55: 49–70.

Blasco F. Model based predictive control using heuristic optimization techniques. Application to non-linear and multivariable processes. Ph.D. thesis, Polytechnic University of Valencia, Spain; 1999.

Boaventura J. Greenhouse climate models: An overview. 4th EFITA Conference 2003; 823–829.

Boulard T, Draoui B. Natural ventilation of greenhouse with continuous roof vents: measurements and data analysis. Journal of Agricultural Engineering Research 1995; 61: 27–36.

Chisci L, Garulli A, Vicino A, Zappa G. Block recursive parallelotopic bounding in set membership identification. Automatica 1998; 34(1): 15–22.

Coello C, Veldhuizen D, Lamont G. Evolutionary algorithms for solving multi-objective problems. Kluwer Academic Publischers 2002.

Ferreira PM, Ruano AEB, Faria EA. Design and implementation of a real-time data acquisition system for the identification of dynamic temperature models in a hydroponic greenhouse. ISHS Acta Horticulturae 519: XXV International Horticultural Congress, Part 9: Computers and Automation, Electronic Information in Horticulture 2000.

Fogel E, Huang F. On the value of information in system identification-bounded noise case. Automatica 1882; 18(12): 229–238.

Herrero JM, Blasco X, Martínez M, Ramos C. Non-linear robust identification using multiobjective evolutionary algorithms. Lecture Notes in Computer Science. Springer-Verlag 2005; 3562: 231–241.

Herrero JM. Robust identification of non-linear systems using evolutionary algorithms. Ph.D. thesis, Polytechnic University of Valencia, Spain; 2006.

Jolliet O, Bailey B. The effect of climate on tomato transpiration in greenhouses: measurements and models comparison. Agric. Forest. Meteor. 1992; 58: 43–62.

Keesman KJ, Stappers R. Non-linear set-membership estimation: A support vector machine approach. J. Inv. Ill-Posed Problems 2004; 12(1): 27–41.

Keesman KJ. Bound-based identification: non-linear-model case. In H. Unbehauen, editor, Encyclopedia of Life Science Systems article 6.43.11.2. UNESCO EOLSS, 2003.

Ljung L. System Identification, Theory for the user. 2nd ed. Prentice-Hall; 1999.

Martínez M, Blasco X, Herrero JM, Ramos C, Sanchis J. Monitorization and control processes. A theorical and practical vision applied to greenhouses. Revista Iberoamericana de Automática e Informática Industrial 2005; 2(4):

5–24.

Milanese M, Norton J, Piet Lahanier H, Walter E. Bounding approaches to system identification. New York: Penum Press 1996.

Milanese M, Vicino A. Estimation theory for non-linear models and set membership uncertainty. Automatica 1991; 27(2): 403–408.

Monteith J. Principles of environmental physics. Contemporary biology. Edward Arnold Ed., UK; 1973.

Reinelt W, Garulli A, Ljung L. Comparing different approaches to model error modelling in robust identification. Automatica 2002; 38(5): 787–803.

Rodríguez F. Modelling and hierarchical control of crop growing in greenhouse. Ph.D. thesis, University of Almería, Spain; 2002.

Rodríguez F, Yebra LJ, Berenguel M, Dormido S. Modelling and simulation of greenhouse climate using Dymola. 5th World Congress of IFAC, Barcelona, Spain, 2002.

Seginer I. The Penman-Monteith evapotranspiration equation as an element in greenhouse ventilation design. Journal of Agricultural Engineering Research 2002; 82(4): 423–439.

Stanghellini C, de Jong T. A model of humidity and its applications in a greenhouse. Agricultural and Forest Meteorology 1995; 76: 129–148.

Ursem U. Diversity-guided evolutionary algorithms. Proc. of Parallel Problem Solving from Nature 2002; 462–471.

Walter E, Piet-Lahanier H. Estimation of parameter bounds from bounded-error data: A survey. Mathematics and Computers in Simulation 1990; 32: 449–468.

Walter E, Pronzalo L. Recursive robust minmax estimation for models linear in their parameters. In Proc. of the IFAC Symposium on Identification and System Parameter Estimation 1991; 1: 763–768.

Walter E, Pronzalo L. Identification of parametric models from experimental data. Springer; 1997.

Walter E, Kieffer M. Interval analysis for guaranteed non-linear parameter estimation. In Proc. of the 13th IFAC Symposium on System Identification 2003.

Figure captions

Figure 1. Multimodal optimization example. $L = 1$, $D \in [0 \dots 1]$, $n\_box = 9$ is the number of boxes in which search space is divided and so the box width is $\epsilon = 1/9$, $J^* = 0.01$ and $\Theta^* := \{\theta \in [0.2 \dots 0.8]\}$. A possible Θ^*_ϵ is represented by means of $\circ$. Note that inside the box, the solution nearest to its centre is preferred - so improving the characterization.

Figure 2. The minimum bounds η_1^{min} and η_2^{min} and $\mathbf{J}(\hat{\mathbf{\Theta}}_{Pr})$ which depend on the selected bounds $\eta_1 > \eta_1^{min}$ and $\eta_2 > \eta_2^{min}$.

Figure 3. Validation process. On the left, the FPS_{ide} is validated, since $FPS \neq \emptyset$. On the right, the FPS_{ide} is invalidated since $FPS = \emptyset$.

Figure 4. Greenhouse climatic model.

Figure 5. $k_j = f(\hat{H}R_i(t_j))$. $\hat{H}R_i(t_j)$ inside relative humidity at sample t_j.

Figure 6. Projections of the Pareto front $\mathbf{J}(\hat{\mathbf{\Theta}}^*_P)$ on different planes $(N_1(\theta), N_2(\theta))$, $(N_1(\theta), N_3(\theta))$, $(N_1(\theta), N_4(\theta))$, $(N_2(\theta), N_3(\theta))$, $(N_2(\theta), N_4(\theta))$ and $(N_3(\theta), N_4(\theta))$.

Figure 7. Each line represents a model of FPS^*_{ide} inside the search space. The horizontal axis represents the seven parameters of each model, whereas the vertical axis shows the parameter values in % with respect to the limits of their search space.

Figure 8. $Y_{ide}(t)$ and the FPS^*_{ide} models envelope.

Figure 9. $Y_{val1}(t)$, $Y_{val2}(t)$ and the FPS^*_{ide} models envelope.

Figure 10. $Y_{val3}(t)$, $Y_{val4}(t)$ and the FPS^*_{ide} models envelope.

Figure 11. $U_{ide}(t)$ identification data corresponding to data collected on 11th (left) and 15th (right) June 2002.

Figure 12. $U_{val1}(t)$, $U_{val2}(t)$, $U_{val3}(t)$, $U_{val4}(t)$ validation data corresponding to data collected on 20th June, 28th July, 22nd August and 8th September 2002 (from left to right).

θ_i	$\frac{\Delta N_1}{\Delta \theta_i}$	$\frac{\Delta N_2}{\Delta \theta_i}$	$\frac{\Delta N_3}{\Delta \theta_i}$	$\frac{\Delta N_4}{\Delta \theta_i}$
gws_{max}	0.12	0.2	0.6	6
gws_{min}	0.15	4	0.8	8
k	0.04	0.8	0.2	3
L	0.8	6	1.5	22
gwb	0.3	6	1.3	10
τ	3	5	10	13
a	0.5	5	1.7	13
G_0	0.2	3	0.8	5
A_c	1	1	3.8	3
C_m	0.05	0.4	0.3	0.5
h_m	0.4	0.6	3	4
T_{ref}	0.004	0.05	0.05	0.2
α_m	0.003	0.04	0.01	0.1
k_a	0.02	0.07	0.06	0.1
fog_{max}	0.6	4	3	30

Table 1

Variation of N_1, N_2, N_3 and N_4 norms when each parameter is independently modified, respect to θ^{ideal}, along its search space.